

ANALYSIS OF A SAMPLED DATA SYSTEM FOR THE OPTIMAL DIGITIZING OF ANALOG FILTERS

Grigore I. Braileanu

Gonzaga University

ABSTRACT

The paper develops the analytical foundation for two IIR filter design methods that have been previously conceived as numerical algorithms for the approximation of analog filters: the extended window digitizing (EWD) method and the matched-pole (MP) frequency sampling design. The derivation of the EWD equations is based on a sampled data system representation, and provides a rigorous foundation for the MP method. Also, an original analysis of a previously proposed optimization process is done by using the equations developed for the sampled data system.

Index Terms — IIR filters, approximation algorithms, signal reconstruction, variable fractional delay

1. INTRODUCTION

The continuous increase of the computing power during the last two decades led to a flurry of activity in the field of optimal design of IIR filters with arbitrary magnitude and phase responses. Yet, the present paper focuses on the field of optimal digitizing of analog filters where very little work has been previously done. In this direction, it is worth mentioning [1] and [2, pp. 515–519], which use the weighted least squares (WLS) minimization, as well as [3, pp. 218–221] which presents a frequency sampling technique. There is no final answer to this problem so far, since imposing arbitrary magnitude and phase responses leads to difficult problems related to the algorithm convergence, filter stability, and the need for a trial-and-error selection of the appropriate weighting function. At the same time, there is an increased interest in a different direction: the incommensurate fractional sampling rate conversion and the related problem of variable fractional delay (VFD) filter design [4]. This requires some form of signal reconstruction from discrete signals under the assumption of bandwidth limitation. Yet, since the output samples are obtained by processing finite sets of data, the inherent signal truncation enlarges the actual bandwidth and produces large errors toward the ends of each new reconstruction interval. Traditionally, this problem is alleviated by taking the middle sample of the current interval as the current output, thus introducing a large delay equal to half the entire reconstruction interval [4]–[6]. Clearly, the delay cannot be made arbitrarily short without affecting the precision.

A different solution to the VFD problem [7] is based on a by-product of the IIR filter design with the so-called extended window digitizing (EWD) method [8], illustrated in Figs. 1 and 2(a) below. In Fig. 1, an $(m+1)$ -point trigonometric interpolator, TI, and the analog prototype H_A are combined into just one sampled data system with the same number of system modes as H_A . To this end, each output segment $y(t)$, $k-1 < t \leq k$, shown in Fig. 2(a) with thick solid line, is generated recursively from the response $y(t)$ of the

analog prototype H_A to the (virtual) signal $x_{TI}(t)$ that interpolates the last $(m+1)$ input samples up to the current time k . The method is characterized by the fact that the auxiliary conditions needed to calculate the response $y(t)$ of $H_A(s)$ are selected as the amplitudes of the last n_A output samples $\{y(k-1), \dots, y(k-n_A)\}$. This provides a natural match for the initial conditions of the analog and digital filters, and so it incorporates the interpolation step into the s - to z -domain mapping step. Thus, the two internal blocks TI and H_A in Fig. 1 are processed as an *entity*, as opposed to [5], [6] which use a cascade connection of the input interpolator and the prototype. Moreover, at each current time k , the *intersample* segment, shown in Fig. 2(a) with a thick line is available for VFD applications.

This sampled data approach to the VFD problem assumes that the necessary fractional delay is to be obtained at the output of a filter. Such a filter may be already required by the system, or needs to be built anyway, as a VFD filter. Instead, this filter is now designed in analog form first, and then digitized with the EWD method. At the same time, the design of analog filters is a well-established subject that includes not only closed form solutions and highly advanced analog approximation techniques, but also well-tested computer programs to carry out the designs. Also, many applications are defined in terms of analog models but are implemented digitally for better accuracy and reliability.

The above features of the EWD method let the designer determine the conventional IIR filter equation, together with a set of equations that approximate some desired intersample output [7]. As these equations are strongly interrelated, their optimization reduces to the minimization of the digitizing error of the IIR filter. Yet, the basic algorithm [8] is time consuming. The solution to this problem was provided by the alternative derivation of the EWD filter with the matched-pole (MP) frequency sampling method, previously proposed in [9]. The IIR filters designed with the MP method were shown to be equivalent to the EWD filters, and then a fast optimization algorithm based on the MP design was presented in [10]. Thus, the optimal design is to be done with the simple and efficient frequency-domain MP method, whereas the more complex time-domain EWD procedure is to be used only when intersample values of the filtered signal are needed. Finally, in contrast to the WLS procedure, which relies on a “good guess” of the weighting function, the MP optimization is straightforward.

The paper is organized as follows. The derivation of the EWD equations based on its sampled data system representation is done in Section 2. The result provides a rigorous foundation for the so-called matched-pole (MP) frequency sampling method, previously proposed in [9]. The MP filter design method is briefly presented in Section 3. Then, an original analysis of the optimization process, previously proposed in [10], is done in Section 4 by using the equations developed in Sections 2 and 3 for the sampled data system. The concluding Section 5 summarizes the main contributions of the paper.

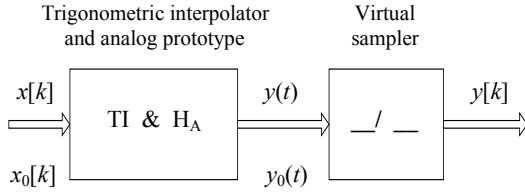


Fig. 1. Block diagram illustrating the EWD method.

2. DERIVATION OF THE EWD EQUATIONS

Throughout the paper, the time is normalized to the sampling period, and so the folding frequency is $\omega_f = \pi/T = \pi$. The signals $x(t)$ and $y(t)$ are the input and output of the analog filter defined by

$$H_A(s) = \frac{Y(s)}{X(s)} = \frac{b(s)}{a(s)} = \frac{b(s)}{s^{n_A} + a_1 s^{n_A-1} + \dots + a_{n_A}}, \quad (1)$$

where $b(s)$ and $a(s)$ are known polynomials, and the roots of $a(s)$ are assumed to be simple (real or complex). The digitizing problem consists in finding a transfer function,

$$H_D(z) = \frac{Y_D(z)}{X_D(z)} = \frac{f(z)}{g(z)} = \frac{f_0 + f_1 z^{-1} + \dots + f_m z^{-m}}{1 + g_1 z^{-1} + \dots + g_{n_A} z^{-n_A}} \quad (2)$$

such that the frequency response $H_D(e^{j\omega})$ represents a “good approximation” of $H_A(j\omega)$. The input and output of the designed digital filter are denoted below by $x_D[k]$ and $y_D[k]$, respectively, while the sampled values of $x(t)$ and $y(t)$ are $x(k)$ and $y(k)$. The block TI & H_A in Fig. 1 is a sampled data system with discrete input $x[k]$ and continuous output $y(t)$.

In its original form, the EWD method is implemented as a numerical approximation [8] which leads to the conjecture that the polynomials $a(s)$ and $g(z)$ in (1) and (2) are given by the relations

$$a(s) = \prod_{n=1}^{n_A} (s - s_n), \quad g(z) = \prod_{n=1}^{n_A} (1 - e^{s_n} z^{-1}). \quad (3)$$

The reason that this method is referred to as the EWD is that, at each current time k , the *interpolation time window* extends to the left of the current time k along a segment of length $m \geq n_A$. Nevertheless, it is worth noting that the actual interpolation is transparent to the designer, as proven in Section 2.1 below by the derivation of the EWD equations. Moreover, these equations prove that the expression of $g(z)$ in (3) is rigorous.

2.1. Impulse Response of the Sampled Data System

In the following, m is odd for the sake of a more concise presentation. The interpolation space is spanned by $2M$ linearly independent functions $\{\cos \omega_n t, \sin \omega_n t\}$, $n = 1, \dots, M$, where $M = (m+1)/2$ or, equivalently, by the exponentials $e^{j\omega_n t}$ and $e^{-j\omega_n t}$, $n = 1, \dots, M$. The *frequency nodes* $\{\omega_n | 0 < \omega_1 < \dots < \omega_M = \omega_{\max} < \pi\}$ are selected according to the procedure developed in [10], and grouped in the vector $\mathbf{w} = [-\omega_M, \dots, -\omega_1, \omega_1, \dots, \omega_M]$ of length $2M = m+1$. Then, the function $x_{TI}(t)$ that interpolates the current set of $(m+1)$ input samples is represented by the expression

$$x_{TI}(t) = \sum_{n=1}^{m+1} \xi_n e^{j\omega_n t}, \quad k-m \leq t \leq k. \quad (4)$$

The coefficients ξ_n are related to the input samples $x(\ell)$ as the unique solution of the linear algebraic equations

$$\sum_{n=1}^{2M} \xi_n e^{j\omega_n \ell} = x(\ell), \quad \ell = k-m, \dots, k. \quad (5)$$

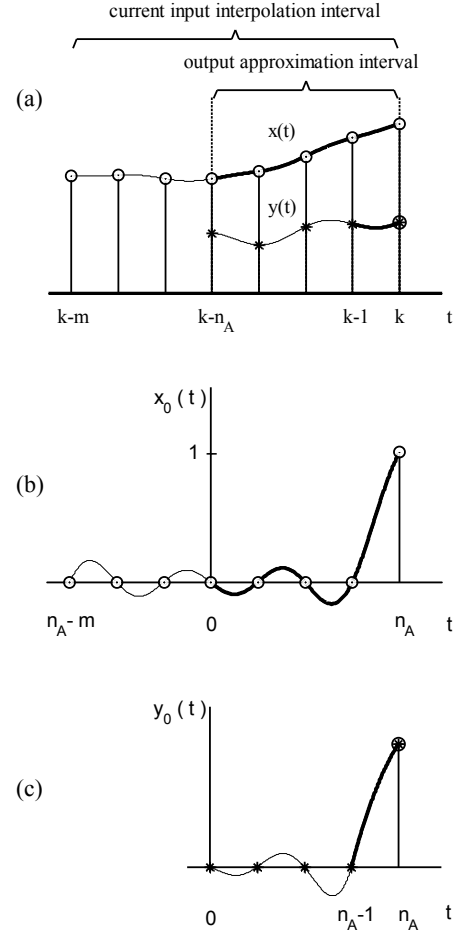


Fig. 2. Input and output signals of the sampled data system ($n_A = 4$, $m = 7$). (a) Interpolated input, $x(t)$, and the output $y(t)$; (b) the eigenfunction $x_0(t)$ of the TI block; (c) the response $y_0(t)$ of the sampled data system to $x_0(t)$.

In order to implement the previously defined auxiliary conditions $\{y(k-1), \dots, y(k-n_A)\}$ of the analog block H_A with the unilateral z - and Laplace transforms, the time origin is temporarily selected such that the discrete input impulse is applied at $t = n_A$. Then, the first nonzero segment of the impulse response $h_{sd}(t)$ of the sampled data system occurs on the time segment $[n_A-1, n_A]$. The expression of the Laplace transform $h_{sd}(s)$ of $h_{sd}(t)$ is derived below by using the particular eigenfunction of TI, $x_0(t)$, defined in the interpolation space as a function with zeros at n_A-m, \dots, n_A , as shown in Fig. 2(b). It is worth noting that $x_0(t)$ and $x_0[k]$ can be expressed as linear combinations of the functions $e^{j\omega_n t}$ and $e^{j\omega_n k}$, respectively, with the same coefficients, ξ_n^0 , $n = 1, \dots, m+1$. The z -transforms of the $(m+1)$ terms of the sampled sequence $x_0[k]$ provide the z -transform $X_D^0(z)$ with a denominator of degree $(m+1)$. At the same time, the delay property and the initial value theorem of the z -transform require

$$\lim_{z \rightarrow \infty} z^{n_A} X_D^0(z) = 1, \quad \text{and} \quad \lim_{z \rightarrow \infty} z^k X_D^0(z) = 0, \quad k = 1, \dots, n_A - 1,$$

for consistency with the condition that the m samples prior to $k = n_A$ are zero.

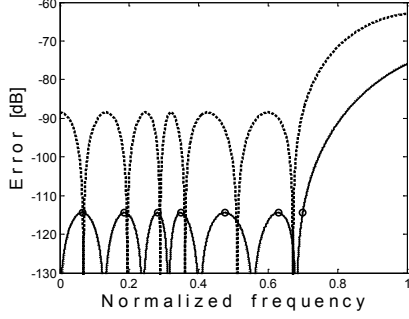


Fig. 3. Digitizing errors, $|E(\omega)|_{\text{dB}}$, for the lowpass analog filter

$$H_A(s) = \frac{0.0033(s^2 + 12.26)(s^2 + 4)(s^2 + 2.69)}{(s+0.768)(s^2+0.23s+0.967)(s^2+0.735s+0.86)(s^2+1.27s+0.686)}.$$

EWD design with $\tau=0$ (dotted line), and optimal EWD for $\tau=0.365$ (solid line). The circles emphasize the EWD equiripple feature.

Thus, the z -transform of $x_0[k]$ becomes

$$X_D^0(z) = \frac{z^{-n_A}}{\prod_{n=1}^{m+1} (1 - e^{j\omega_n} z^{-1})} \triangleq \frac{z^{-n_A}}{q_D(z)}, \quad q_D(z) = 1 + \dots + q_m z^{-m}, \quad (6)$$

and does not even require the knowledge of the coefficients ζ_n^0 . Then, the coefficients ζ_n^0 are uniquely defined by the partial-fraction expansion of the rational function in (6). As the poles of $X_0(z)$ are simple, a tedious but straightforward computation yields the complex coefficients ζ_n^0 and, finally, the real form of the Laplace transform of $x_0(t)$,

$$X_0(s) = \sum_{n=1}^{m+1} \frac{\zeta_n^0}{s - j\omega_n} = \sum_{n=1}^M \frac{\alpha_n s + \beta_n^0}{s^2 + \omega_n^2} \triangleq \frac{p(s)}{q(s)}, \quad (7)$$

where

$$\alpha_n^0 = \frac{\sin(M - n_A)\omega_n}{\rho_n \sin \omega_n}, \quad \beta_n^0 = \frac{\cos(M - n_A)\omega_n}{\rho_n \sin \omega_n}, \quad (8)$$

$$\rho_n = 2^{M-1} \prod_{\substack{\ell=1 \\ \ell \neq n}}^M (\cos \omega_n - \cos \omega_\ell), \quad n = 1, \dots, M.$$

Since $x_0(t)$ is *exactly interpolated* from any consecutive $(m+1)$ samples in $x_0[k]$, the zero-state response of the analog model H_A can be obtained from the Laplace transform $Y_{zs}(s) = X_0(s)H_A(s)$, whereas the actual response $y_0(t)$ of the sampled data system TI& H_A requires the additional *zero-input component*, $y_{zi}(t)$, corresponding to the *auxiliary conditions*, which are n_A consecutive zeros, as illustrated in Fig. 2(c). Apparently, the denominator of $Y_{zi}(s)$ is $a(s)$, and so the Laplace transform of the total response $y_0(t)$ becomes

$$Y_0(s) = X_0(s)H_A(s) + Y_{zi}(s) = \frac{p(s)b(s)}{q(s)a(s)} + \frac{c_{zi}(s)}{a(s)}, \quad (9)$$

where the n_A coefficients of the polynomial $c_{zi}(s)$ will be determined in Section 2.2 below, and the other four polynomials were defined above by (1), (7), and (8).

Now, let $h_{sd}(t)$ be the response of the sampled data system to the discrete impulse $\delta[k]$, and assume that the input of the sampled data system is $x_0[k]$ — the sampled eigenfunction of the interpolator TI. Then, the total response $y_0(t)$ to $x_0[k]$, can be also written as $y_0(t) = \sum_{\ell=0}^{\infty} x_0[\ell]h_{sd}[t - \ell]$, which yields an alternative form of (9), $Y_0(s) = \sum_{\ell=0}^{\infty} x_0[\ell]e^{-\ell s}H_{sd}[s] = X_D^0(e^s)H_{sd}[s]$, where $X_D^0(e^s)$ is the z -transform (6) of $x_0[k]$ with z replaced by e^s .

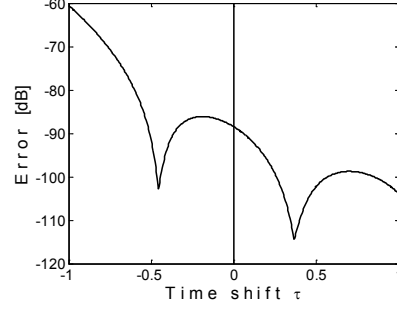


Fig. 4. The Chebyshev norm $\|E(\omega)\|$ plotted as a function of the time shift τ for the EWD design illustrated in Fig. 3 ($\tau_{\text{opt}}=0.365$).

Finally, the Laplace transform of the impulse response of the sampled data system is given by

$$H_{sd}(s) = \frac{Y_0(s)}{X_D^0(e^s)} = e^{s n_A} q_D(e^s) \left(\frac{p(s)b(s)}{q(s)a(s)} + \frac{c_{zi}(s)}{a(s)} \right). \quad (10)$$

2.2. Transfer Function of the EWD Filter

According to Fig. 1, the output of the digital IIR equivalent to the analog prototype H_A is the sampled output of the sampled data system TI& H_A . While the latter is a linear periodically time-varying system with period $T=1$ and does not have a transfer function, the resulting discrete time system is time invariant with a transfer function that can be obtained directly from (10),

$$H_D(z) = Z\{h_{sd}[k]\} = z^{n_A} q_D(z) Z\left\{ \frac{p(s)b(s)}{q(s)a(s)} + \frac{c_{zi}(s)}{a(s)} \right\}, \quad (11)$$

where the symbolic notation $Z\{Y(s)\} = Z\{L^{-1}[Y(s)]|_{t=k}\}$ represents the z -transform of the samples of $y(t)$. This is done with the traditional the s - to z -domain transformation based on the partial-fraction expansion of rational functions. The two factors $a(s)$ and $g(s)$ in the denominator become $g(z)$ and $q_D(z)$, respectively, as defined in (3) and (6). Thus, (11) becomes

$$H_D(z) = z^{n_A} \left(\frac{\mu_0 + \dots + \mu_{m+n_A} z^{-m-n_A}}{g(z)} + \frac{q_D(z)(\gamma_1 + \dots + \gamma_{n_A} z^{-n_A})}{g(z)} \right)$$

where the only unknown coefficients are $\gamma_1, \dots, \gamma_{n_A}$. In order to obtain the final (causal) expression (2) of $H_D(z)$, these coefficients are calculated such that the first n_A leading terms of the numerator are canceled. This requirement is satisfied by the following recursive equations:

$$\gamma_1 = -\mu_0, \quad \left\{ \gamma_n = -\mu_{n-1} - \sum_{\ell=1}^{n-1} q_\ell \gamma_{n-\ell} \right\}, \quad n = 2, \dots, n_A.$$

Now, the partial-fraction expansion of the rational function

$$Y_{zi}(z) = Z\left\{ \frac{c_{zi}(s)}{a(s)} \right\} = \frac{\gamma_1 + \dots + \gamma_{n_A} z^{-n_A}}{g(z)} = \sum_{n=1}^{n_A} \frac{c_n}{1 - z^{-1} e^{s_n}} \quad (12)$$

is mapped back into the s -domain to provide the polynomial $c_{zi}(s)$:

$$\sum_{n=1}^{n_A} \frac{c_n}{1 - z^{-1} e^{s_n}} \implies \sum_{n=1}^{n_A} \frac{c_n}{s - s_n} = \frac{c_{zi}(s)}{a(s)}. \quad (13)$$

In conclusion, the derivation of Eqs. (10)–(13) proves that the EWD filter is described by a transfer function of the form (2) with the denominator $g(z)$ rigorously defined in (3).

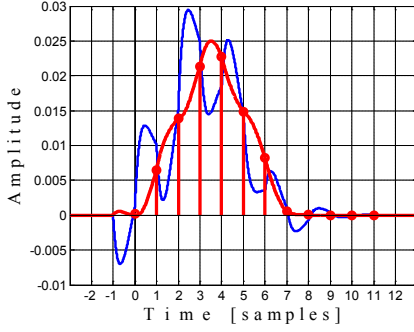


Fig.5. Inverse Laplace transforms of $g(e^s) e^{-\tau s} H_{sd}(s)$ with effective widths 11 for $\tau = 0$ (thin line), and 7 for the optimal value $\tau = 0.365$ (thick line). The stems show the m coefficients of the optimal filter as samples of the inverse Laplace transform.

3. MATCHED-POLE FREQUENCY SAMPLING DESIGN

The matched-pole (MP) frequency sampling method for IIR filter design was shown in [9] to be equivalent with the design of the basic EWD filter transfer function (2) based on the relationships (3) which were proposed as a conjecture. Now, in the light of the above conclusion of Section 2, the proof of the EWD-MP equivalence [9] becomes rigorous. Briefly stated, the digitizing of filters by frequency sampling is reduced only to the computation of the numerator $f(z)$ in (2), while the denominator $g(z)$ is fixed and defined by (3). The design parameters are $m > n_A + 1$ (an odd number), $M = (m+1)/2$ and the frequency nodes $\{\omega_n | 0 < \omega_1 < \dots < \omega_M = \omega_{\max} < \pi\}$ which are determined according to the procedure developed in [10]. Thus, $(m+1)$ equations

$$f(e^{j\omega_n}) = H_A(j\omega_n) g(e^{j\omega_n}), \quad n = \pm 1, \dots, \pm M, \quad (14)$$

are to be solved for the unknown $(m+1)$ coefficients of $f(z)$.

With the poles of $g(z)$ rigorously matched to those of $a(s)$, the IIR filter design has become an FIR frequency-sampling problem referred to as the *matched-pole frequency sampling design*.

4. ANALYSIS OF THE OPTIMAL PROPERTIES OF THE SAMPLED DATA SYSTEM

Since the sampled data system analyzed in Section 2 is a linear periodically time-varying system with period $T=1$, the output depends on the particular time instant within one sampling period when the current input sample ($x[k]$ in Fig. 2(a)) is applied. Based on this fact, it is argued in [10] that time shifts of length $-1 < \tau < 1$ are equivalent to adding a group delay τ to the analog prototype that may be beneficial to the accuracy of the digitizing process. Now, the MP equations simply become

$$f(e^{j\omega_n}) = e^{-j\tau\omega_n} H_A(j\omega_n) g(e^{j\omega_n}), \quad n = \pm 1, \dots, \pm M, \quad (14')$$

and the implementation of this delay in the equations derived in Section 2 above requires only the change of α_n^0 and β_n^0 in (8) to

$$\alpha_n^\tau = \frac{\sin(M - n_A - \tau)\omega_n}{\rho_n \sin \omega_n} \quad \text{and} \quad \beta_n^\tau = \frac{\cos(M - n_A - \tau)\omega_n}{\rho_n \sin \omega_n}$$

with the subsequent modifications of the polynomial $p(s)$.

4.1. Optimal Equiripple EWD/MP Design

The optimization developed in [10] is done with the MP fast algorithm that solves (14') for the $(m+1)$ real coefficients of $f(z^{-1})$ and minimizes the Chebyshev norm,

$$\|E(\omega)\| = \max_{0 < \omega < \omega_{\max}} |E(\omega)|, \quad (15)$$

of the digitizing error,

$$E(\omega) = \frac{f(e^{j\omega})}{g(e^{j\omega})} - e^{-j\tau\omega} H_A(j\omega), \quad (16)$$

where ω_{\max} is predetermined, $g(z)$ is given by (3), and τ is to be obtained in the final stage of the optimization. The example presented in [10] is used below in order to assess the results of Section 2. Fig. 3 shows typical plots of $|E(\omega)|_{dB} = 20 \log_{10} |E(\omega)|$, corresponding to $\tau = 0.365$, $m = 11$, and $\omega_{\max} = 0.7\pi$. The optimization, illustrated in Fig. 4, is performed by repeatedly running the MP algorithm for values of τ within the interval $[-1, 1]$ and plotting $\|E(\omega)\|$ as a function of τ . Typically, this plot is very smooth and has a single minimum in the interval $[0, 1]$.

4.2. Main Property of the EWD/MP Design

There is a conceptual difference between the MP frequency interpolation (14) and the frequency sampling method that is used in [3, pp. 218–221] to find a discrete transfer function (2) whose frequency response interpolates a given complex expression $H_A(j\omega)$ at equally spaced frequency points. The better performance of the MP method is directly related to the particular choice of the function to be approximated, typical of digitizing methods. Accordingly, the well-defined denominator $g(z)$ leads to the approximation of the function $H_{MP}(s) = g(e^s) H_{sd}(s)$ which, unlike $H_A(s)$, is an *entire function* of s and its inverse Laplace transform has compact support [11, Theorem 10–6] with width equal to $(m+1)$ [10]. Specifically, the factors of $H_{MP}(s)$ are of the form

$$\frac{1 - e^{-(s-p_n)}}{s - p_n} \quad \text{and} \quad \frac{1 - e^{-(s-j\omega_n)}}{s - j\omega_n},$$

and are entire functions due to the pole-zero cancellations. It follows that the fundamental difference between the direct interpolation [3] and the FIR-like interpolation (14) stems from the dual form of the Nyquist-Shannon sampling theorem [2], [12], where ω is viewed as a “time variable” whereas t becomes a “frequency variable.” Thus, the above derivations show that the conditions of the sampling theorem are far from being satisfied by the method described in [3], where $h_A(t) = L^{-1}\{H_A(s)\}$ extends over an excessively wide time segment, but are fully satisfied by the MP design since $h_\tau(t) = L^{-1}\{g(e^s) e^{-\tau s} H_{sd}(s)\}$ is strictly “bandlimited” being zero outside an interval of finite length [12]. This fact is illustrated in Fig. 5 where $h_\tau(t)$, computed numerically for the system in Fig. 3, exhibits an effective width of 11 samples for $\tau = 0$ and 7 samples for $\tau = 0.365$.

5. CONCLUSIONS

The paper derived the exact equations of EWD and MP filters for both the conventional design and the design with a delay τ ($\tau < 1$) which amounts to digitizing $e^{-\tau s} H_A(s)$ rather than $H_A(s)$. While this modification only slightly increases the inherent group delay of $H_A(s)$ by τ , it allows for a dramatic decrease of the digitizing error (usually, by more than one order of magnitude with respect to traditional methods). Also, in contrast to the WLS optimization, which relies on a “good guess” of the weighting function, the MP optimization is straightforward. Finally, based on the EWD/MP identity, the optimal MP parameters can be used by the time-domain EWD design when intersample values of the filtered signal are needed for sampling rate conversion or VFD applications.

6. REFERENCES

- [1] Chen and Parks [1990]: X. Chen and T.W. Parks, "Design of IIR filters in the complex domain," *IEEE Trans. Acoust., Speech, Signal Processing*, vol. 38, pp. 910–920, 1990.
- [2] S. K. Mitra, *Digital Signal Processing. A Computer-Based Approach*, McGraw–Hill, New York, NY, 2006.
- [3] T. W. Parks and C. S. Burrus, *Digital Filter Design*, John Wiley, New York, 1987.
- [4] T. I. Laakso, V. Välimäki, M. Karjalainen, and U.K. Laine, "Splitting the Unit Delay," *IEEE Signal Processing Magazine*, vol. 13, pp. 30–60, 1996.
- [5] M. Unser, "Cardinal Exponential Splines: Part II – Think Analog, Act Digital," *IEEE Trans. Signal Process.*, vol.53, pp. 1439–1449, 2005.
- [6] S. Särkkä, "Accurate Discretization of Analog Audio Filters with Application to Parametric Equalizer Design," *IEEE Trans. Audio, Speech, Language Process.*, vol.19, pp. 2486–2493, 2011.
- [7] G. I. Braileanu, "Digital Filters with Implicit Interpolated Output," *IEEE Trans. Signal Process.*, vol.45, pp.2551–2560, 1997.
- [8] G. I. Braileanu, "Extended–Window Interpolation Applied to Digital Filter Design," *IEEE Trans. Signal Process.*, vol. 44, pp. 457–472, 1996.
- [9] G. I. Braileanu, "Equivalence Between the Extended Window Design of IIR Filters and Least Squares Frequency Domain Designs," *Proc. 2003 Int. Conf. on Acoustics, Speech, and Signal Process. (ICASSP 2003)*, Hong Kong, vol. VI, pp. 21–24, 2003.
- [10] G. I. Braileanu, "Optimal Design of Digital Equivalents to Analog Filters," *Proceedings of the 2010 IEEE Workshop on Signal Processing Systems*, San Francisco Bay Area, CA, pp. 438–443, Oct., 2010.
- [11] W. R. LePage, *Complex Variables and the Laplace Transform for Engineers*, Dover Publications, New York, 1980.
- [12] H. J. Landau, "Necessary Density Conditions for Sampling and Interpolation of Certain Entire Functions," *Acta Math.*, vol. 117, pp. 37–52, Feb.1967.